Kuwait J. Sci. **48 (1)** pp. 59-66, 2021

Optimum design of the hybrid (diffractive/refractive) multifocal intraocular lenses implanted within human eye

Ali H. Al-Hamdani[1,*], Hayfa G. Rashid[2], Hussein T. Hashim[2]

[1]*Dept. of Laser and Optoelectronics, Engineering, University of Technology, Iraq*

[2]*Dept. of Physics, College of Education, University of Al-Mustansiryah, Iraq*

[*]*Corresponding author: 140002@uotechnology.edu.iq*

Abstract

The human eye natural crystalline lens becomes opaque due to cataract. For improvement of the eye vision, the crystalline lens is typically surgically removed and replaced by an intraocular lens (IOLs). The optimum design of hybrid multifocal intraocular lenses (MIOLs) implanted within the human eye model is proposed. The AR40N acrylic MIOLs material has good biocompatibility. Two types of hybrid MIOLs (diffractive/refractive (D/R) and refractive/diffractive (R/D)) with four foci were designed and evaluated. A comparison between the image quality for a healthy eye (Liou & Brennan model) and an eye with the implanted hybrid MIOLs has been performed based on ZEMAX-EE optical software. The image characteristics, point spread function (PSF), modulation transfer function (MTF), blur spot size, and longitudinal chromatic aberration (LCA) were used as an image criterion in this study. The eye pupil diameter was "3 mm," the visual field of view was 5 degrees, and the light spectral region was 455- 655 nm. Results indicate that both hybrid MIOLs models achieved good visual acuity (sharp vision) for distances within the range 25 to 10^8 cm. The MIOLs made a remarkable correction in chromatic aberration than the healthy eye. The MTF for R/D-MIOL model improves the visual quality more than D/R-MIOL and healthy eye models.

Keywords: Diffractive optics; hybrid intraocular lens; image quality; implanted intraocular lens; multifocal intraocular lenses.

1. Introduction

Due to the cataract, the human eye natural crystalline lens becomes opaque. Up to now, the crystalline lens is typically surgically removed and replaced by an intraocular lens (IOLs), which is the only effective method of therapy (Barbero *et al.,* 2011; Dandona *et al.,* 2003; Olofsson *et al*., 2001; Pager *et al*., 2004). Medical statistical estimation indicates that 52.6 million people worldwide are affected by cataract within 33% of total visual impairment and 51% of total blindness (Sieburth and Chen, 2019). Usually, IOLs materials, generally available in three types, which differ in the refraction index and dispersion, are poly (methyl methacrylate) (PMMA), silicone (polydimethylsiloxane), and acrylic (ethyl acrylate) (Packer *et al.,* 2006; Siedlecki *et al*., 2007). The antireflection for the IOLs has been used by Kokaj *et al.* (2018) to protect the retina from ultraviolet light damage. When the IOLs were implanted within the human eye, the retinal image depends on the IOL focusing power and the refractive index (Siedlecki *et al.,* 2008). The phakic and aphakic IOLs are classified into monofocal and multifocal (Packer *et al*., 2006; Weeber *et al*., 2008). Nowadays, multifocal IOLs are widely used. There are several types of IOLs, i.e., refractive (R), diffractive (D), apodized (R/D), and hybrid (R/D) (Siedlecki *et al.,* 2008; Sokolowski *et al*., 2015; Weeber *et al.,* 2008). As shown in Figure 1, refractive and diffractive surfaces have been used by Zając and Nowak (2002) to compose hybrid IOLs microstructure. In the human vision (polychromatic light), both the monochromatic and chromatic aberrations affect the retinal image quality (Siedlecki *et al.,* 2008; Song *et al.,* 2016).

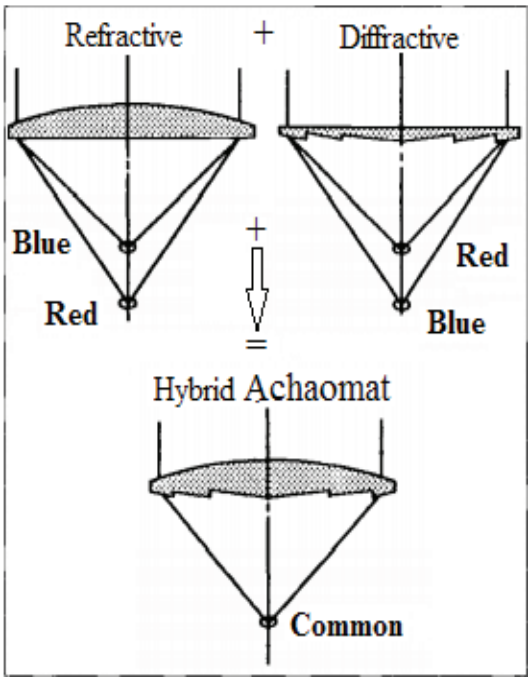

Fig. 1. Principle design of hybrid (refractive-diffractive) lenses (Zając and Nowak, 2002).

A few articles have been concerned with the performance of IOLs in polychromatic light (Weeber *et al.,* 2008).

Recent studies depicted that the improvement of visual acuity and contrast sensitivity may be achieved when the monochromatic and chromatic aberrations were corrected at the same time (Song *et al.,* 2016). Shaker M. L. *et al.* (2020) used different contact lens materials to correct chromatic and polychromatic aberrations.

In this study, the hybrid R/D and D/R MIOLs have been designed based on the AR40N (acrylic) material. These MIOLs are used to correct the chromatic and spherical aberrations. Moreover, the retinal eye sensitivity for different vision wavelengths is included in this study.

2. Material and method

The retinal images quality formed by a healthy eye and eye with MIOLs was adopted with ZEMAX 13 Release 2 optical design software (Zemax, 2014) and laptop characteristics Core i7, 4th Gen/8GB/256 GB SSD/ Windows7,64-bit. Table 1 summarized healthy eye (L.&B. model) parameters of the optical surface. L.&B. model was accepted widely as one of the best approximations of the real optical system of a human eye (it contains features of the biological eye) (Almeida and Carvalho, 2007; Siedlecki *et al.*, 2008).

Table 1. Optical surface parameters of the L.&B. model.

Surf.	Comment	Radius. (mm)	Thickness. (mm)	Glass		Semi-Diameter	Conic
				n at 555 nm	Abbe number		
OBJ	Object	Infinity	Infinity	-	-	0	0.00
1	Anterior cornea	7.77	0.55000	1.376	50.23	5	-0.18
2	Posterior cornea	6.40	3.16000	1.336	50.23	5	-0.60
STO	Pupil	Infinity	0.00000	1.336	50.23	1.25	0
3	Lens- front	12.40	1.59000	Grad A	-		-0.94
4	Lens- back	Infinity	2.43000	Grad P	-	5	0.00
5	Vitreous	-8.10	16.23883	1.336	50.23	5	0.96
IMA	Retina	-12.00	-	-		5	0

* where OBJ, STO, and IMA are object, stop, and image surfaces, and n is the refractive index.

The crystalline lens in the L.&B. model is composed of anterior and posterior surfaces with gradient refractive index. The distribution of gradient index and the index in anterior (n_A) and posterior surfaces (n_P) is given by the following equations (Liou and Brennan, 1997):

$$[n_A(z,r)] = 1.368 + 0.049057z - 0.015427z^2 - 0.001978r^2, \quad (1),$$

$$[n_P(z,r)] = 1.4078 - 0.006605z^2 - 0.001978r^2, \quad (2),$$

Because of the L.& B. model, the dispersion relation can be used to describe all eye media

$$n(\lambda) = n_{555} + 0.0512 - 0.1455\lambda + 0.0961\lambda^2 \quad (3),$$

For this model, the z-axis was oriented along the visual axis of the eye model eye with cylindrical coordinates (z,r). The n_{555} is the material refractive index at 0.555μm incident wavelength.

The proposed design for an achromatic hybrid MIOL is made of acrylic AR40N material with refractive index $n = 1.47$ and Abbe number $V_d = 71$ (Siedlecki *et al.*, 2008). The following relation describes the combination of refractive and diffractive surfaces (López-Gil and Montés-Micó, 2007; Zemax, 2014):

- Aspherical refractive surface (even asphere) with a sagitta (z) of

$$z = \frac{(c\times r^2)}{1+\sqrt{1-(1+k)c^2r^2}} + \alpha_1 r^2 + \alpha_2 r^4 + \alpha_3 r^6 + \alpha_4 r^8 \quad (4),$$

- Aspherical diffractive surface (binary 2) with a sagitta (z) of

$$z = \frac{(c\times r^2)}{1+\sqrt{1-(1+k)c^2r^2}} + \sum_{i=1}^{N} \alpha_i \rho^{2i} \quad (5),$$

$$\phi = M \sum_{i=1}^{N} \alpha_i \rho^{2i} \quad (6),$$

where "c" is the surface curvature, and "r" and "k" are the radial coordinate and conic constant, respectively. N is the number of polynomial coefficients in the series, α_i is the normalized radial coordinate, which represents the coefficient on the i^{2th} power of ρ, and M is the coefficient of diffraction.

The optimum performance of hybrid MIOLs was studied and evaluated with the aid of the ZEMAX program accessed using a merit function defined as (Zemax, 2014)

$$MF = \left[\frac{1}{N}\sum_{j=1}^{N}\left[\frac{f(\lambda_i)-\hat{f_j}}{\Delta\hat{f_j}}\right]^2\right]^{1/2} \quad (7),$$

f, is abbreviated as the actual spectral characteristic of transmittance or reflectance. From a given wavelength grid with the total number of N points, λ_j were selected as wavelength points with target values and specified tolerances $\hat{f_j}$ and $\Delta\hat{f_j}$, respectively.

$$RMS = \frac{\sum_{i=1}^{n}\sqrt{(x_i-x_0)^2+(y_i-y_0)^2}}{N} \quad (8),$$

where N is the total number of rays; (x_0, y_0) and (x_i, y_i) are the reference and the ray intersection points, respectively.

The modulation transfer function (MTF) is a fundamental tool for assessing the performance of imaging systems. Another essential concept is the optical transfer function (OTF) (Wang *et al.*, 2008), (Alemeddine *et al.*, 2002):

$$OTF = MTF\, e^{-j\theta(u,v)} \quad (9),$$

where (u, v) are the coordinates in the frequency domain.

Therefore, the optical transfer function is a spatial frequency-dependent complex variable whose modulus is the modulation transfer function and whose phase is described by the phase transfer function (PTF).

The longitudinal chromatic aberration (LCA) of the eye can be defined as (Wang *et al.,* 2008)

$$LCA = F_R - F_B = \frac{n_R - n_B}{r}, \quad (10),$$

where F_R and F_B are the powers of the eye for two wavelengths (R and B), n_R and n_B are the eye's refractive indices for the two wavelengths, and r is the radius of curvature of the refracting surface. The effective focal length for healthy eye and {(R/D) & (D/R)} hybrid MIOL was 16.58mm, 16.508mm, and 16.414 mm, respectively.

The spectral sensitivity of the retina in the visual region (photopic state) was taken in optimization (de l'Éclairage, 1990; Kaiser and Boynton, 1996) in healthy and hybrid MIOLs implanted eye models. The data of human eye spectral sensitivity are presented in Table 2.

Table 2. The human eye spectral sensitivity.

Wavelength (mm)	**0.455**	**0.505**	**0.555**	**0.605**	**0.655**
Spectral sensitivity	0.0746	0.4027	0.8658	0.4569	0.0568

3. Results and Discussion

The optical performance of the healthy eye and the eye with implanted hybrid MIOLs has been designed and analyzed through computer simulations ZEMAX. The PSF and MTF are used as the criteria to analyze the image of the proposed eyes with 3 mm input pupil diameter and 5° field of view.

Tables 3 and 4 summarize the design parameters of hybrid R/D and D/R MIOLs implanted in the eye, respectively.

Table 3. Optical surface data parameters for hybrid R&D MIOLs.

Element.	**Radius.** (mm)	**Thickness.** (mm)	**Semi diameter.** (mm)	**Refractive index.**	**Even Aspheric Coefficients**		
					Conic constant	**4th order**	**6th order**
Anterior Surface (R)	11.35	0.94	3	1.470	-7.478	8.460E-4	- 1.595E-4
Posterior Surface(D)	-20.84	2.43	3	1.336	-24.688	4.372E-5	- 1.034E-4
Coefficients for Surface (D)	**Norm. Radius**		**Coeff.p^2**		**Coeff.p^4**	**Coeff.p^6**	**Coeff.p^8**
	3		-137.1600		24.4831	2.7308	24. 2186

Table 4. Optical surface data parameters for hybrid D&R MIOLs.

Element.	**Radius.** (mm)	Thickness. (mm)	**Semi diameter**. (mm)	**Refractive index.**	Even Aspheric Coefficients		
					Conic constant	**4th order**	**6th order**
Anterior Surface (D)	33.48	0.90	3	1.470	27.59	-2.22E-3	- 9.74E-5
Posterior Surface (R)	-8.93	2.43	3	1.336	7.26	-1.44E-3	2.65E-4
Coefficients for Surface (D)	**Norm. Radius**		**Coeff.p^2**		**Coeff.p^4**	**Coeff.p^6**	**Coeff.p^8**
	3		-1.27E+2		1.697E+2	-2.97E+2	1.33E+2

Figures 2 depicts the polychromatic PSF of the healthy eye (black color) and eye model with hybrid MIOLs [R/D (blue color) and D/R (red color)] implanted. The results show that the optical performance of polychromatic PSF shapes of the eye model with hybrid MIOLs implanted seems to look like a healthy eye.

The image position was shifted as the MIOL was implemented. Figure 3 indicates that the tangential MTF is better than the sagittal MTF, which indicates that the system is asymmetric. It is also clear that the MTF values for IOLs and healthy eyes are equal to each other until the spatial frequency =30 cycles/mm. After 30 cycles/mm, MTF for R/D MIOL is higher than the MTF for D/R MIOL or the healthy eye.

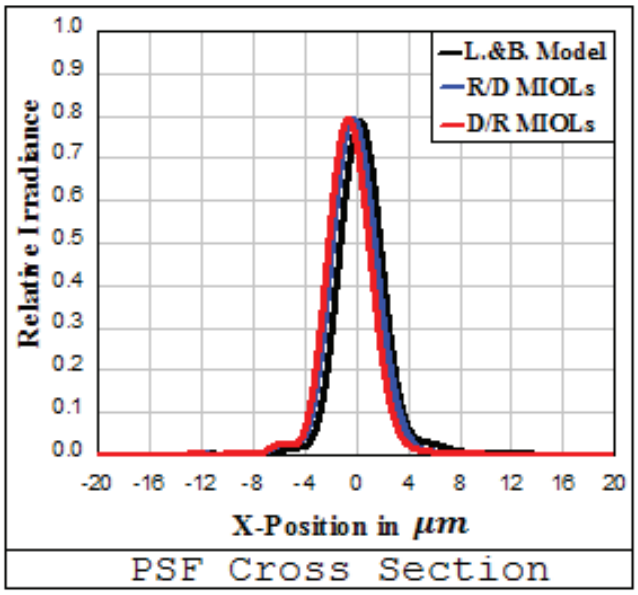

Fig. 2. Polychromatic PSF of the healthy eye and the eye with hybrid MIOLs implanted.

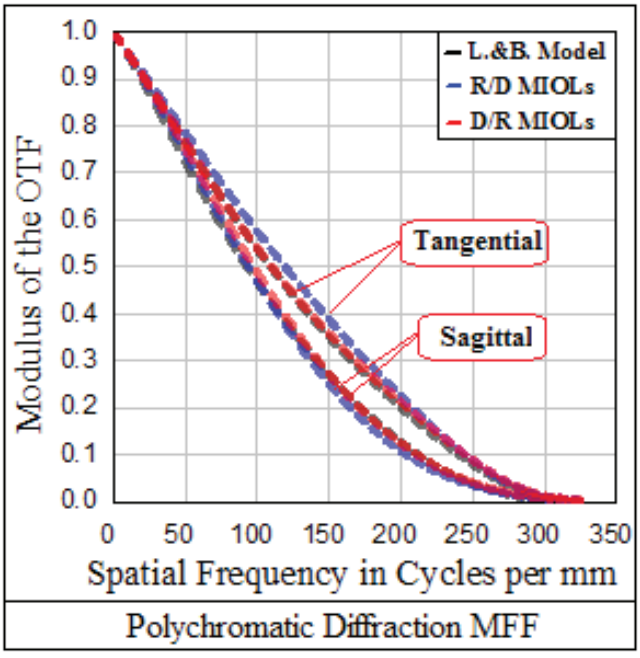

Fig. 3. Polychromatic (Tangential and Sagittal) MTF for the healthy eye and the eye with hybrid MIOLs implanted.

Figure 4 shows the polychromatic spot diagram for the healthy eye and the eye with hybrid MIOLs. The measured RMS radius is 2.67, 1.436, and 1.561μm for the healthy eye, eye with hybrid MIOL R/D, and eye with D/R MOIL, respectively.

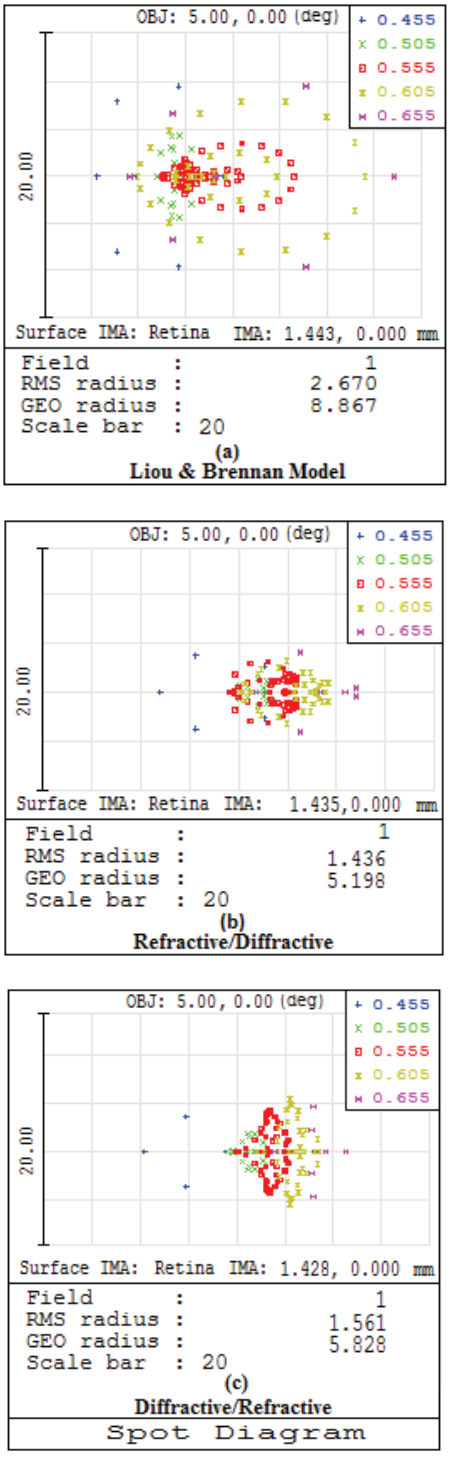

Fig. 4. Polychromatic spot diagram for healthy eye and eye with hybrid MIOLs implanted.

The effect of MIOLs shapes on the amount of spherochromatic (spherical and chromatic) aberration was taken into account in this study. Figures 5 and 6 illustrate the longitudinal chromatic focal shift (LCA) and the longitudinal spherical aberration (LSA) for the healthy eye (a) and the eye with hybrid R/D and D/R MIOLs (b and c, respectively).

It is shown from table 5 that the MIOLs with a diffractive posterior surface will reduce the chromatic LCA more than MIOLs with a rear refractive surface. Also, MIOLs reduce the LCA from 128 µm for the eye without IOLs to 33 and 32 µm for the eye with R/D and D/R IOLs, respectively. Also, there is an additional advantage of hybrid MIOLs implementation concerned with reducing longitudinal spherical aberration that improves the human eye vision.

Table 5. Spot size, LCA, and LSA for different IOLs.

Model	Spot size µm	LCA µm	LSA mm
B.&L.	2.67	128	.176
R/D	1.436	33	.068
D/R	1.561	32	.059

The results show that the proposed hybrid R/D and D/R MIOLs have an excellent correction for chromatic dispersion and spherical aberration.

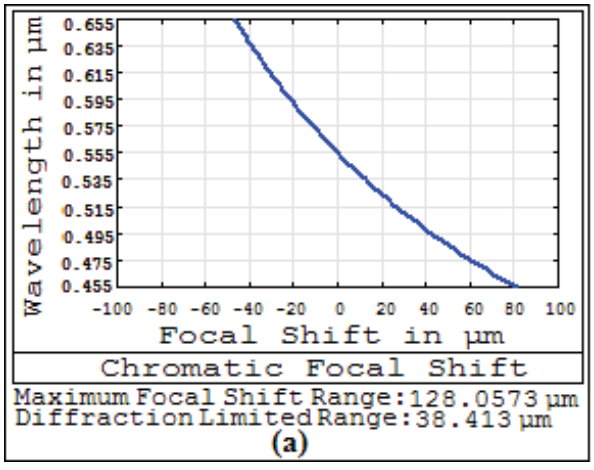

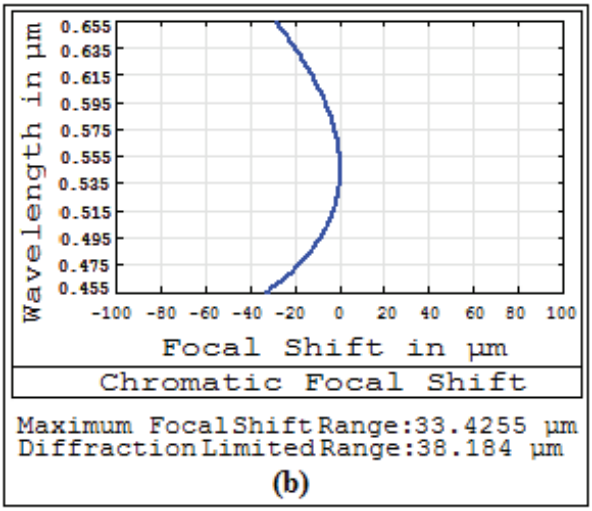

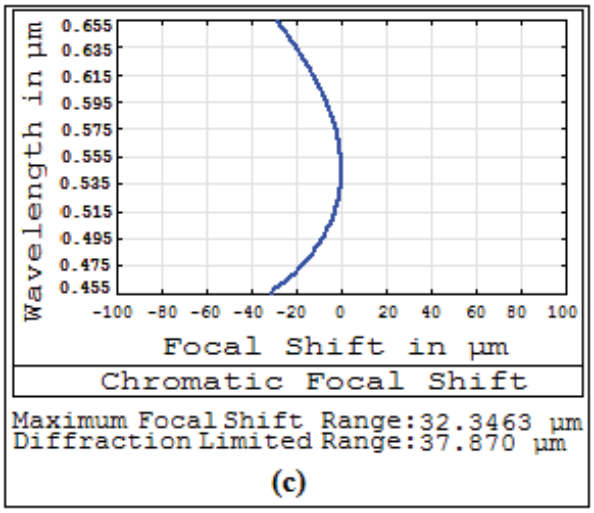

Fig. 5. Longitudinal-chromatic aberration (LAC) of (a) healthy eye, (b) eye with hybrid MIOL R/D, and (c) eye with D/R MOIL.

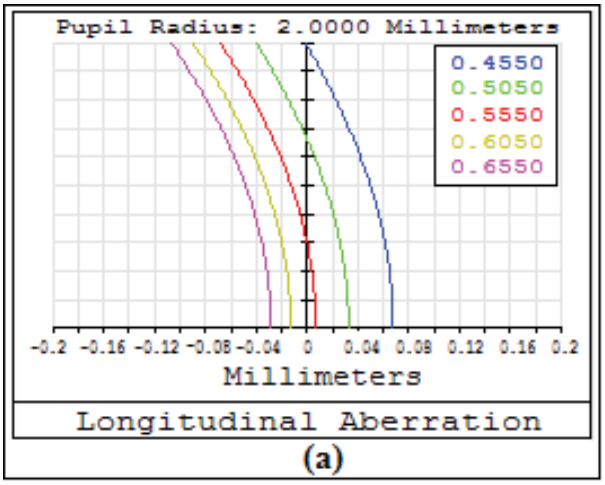

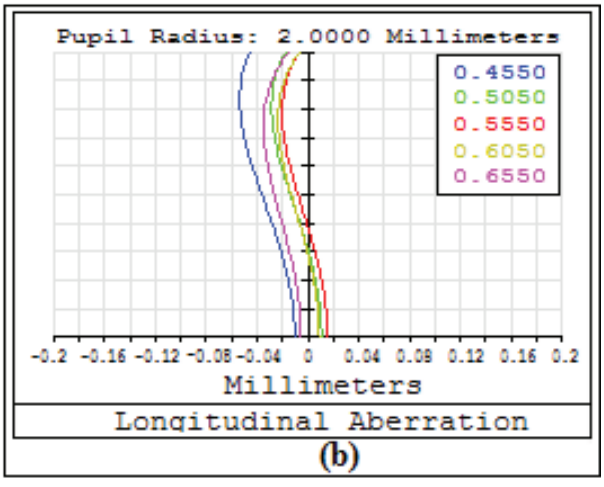

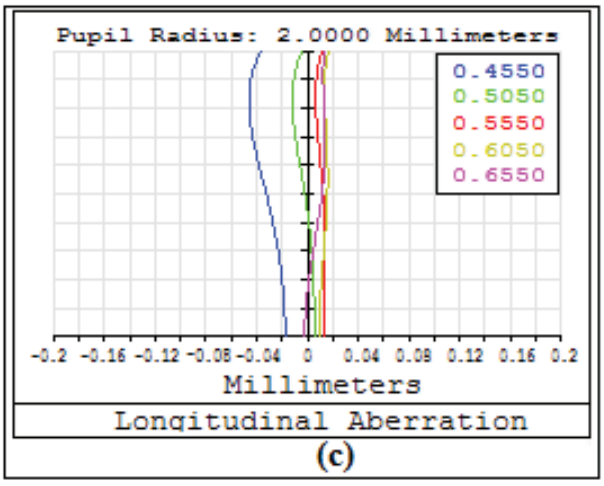

Fig. 6. Spherochromatic aberration of (a) L.&B. model and eye with hybrid MIOLs implanted, (b) R&D model, and (c) D&R model.

Figure 7 illustrates the fifth order spherical aberration (SPHA) for the polychromatic wavelength (0.455, 0.505, 0.550, 0.605, and 0.650μm) for the healthy eye (a) and the eye with hybrid R/D & D/R MIOLs (b and c, respectively). The color ray fan plot dramatically illustrates this. In Figure 7, the green-light plot is lying flat on the x-axis. This means that we are at the green light paraxial focal plane. There is a little bit of curl toward the edge of the pupil due to the fifth order. The blue- and red-light plots are not flat since they are defocused relative to the green-light image plane. But they do have the same slope through the central portion of the plot, which is indicative of the achromatic correction. A little spherical aberration was presented. On the other hand, the blue-light plot shows slightly more third-order spherical and much more fifth-order aberration.

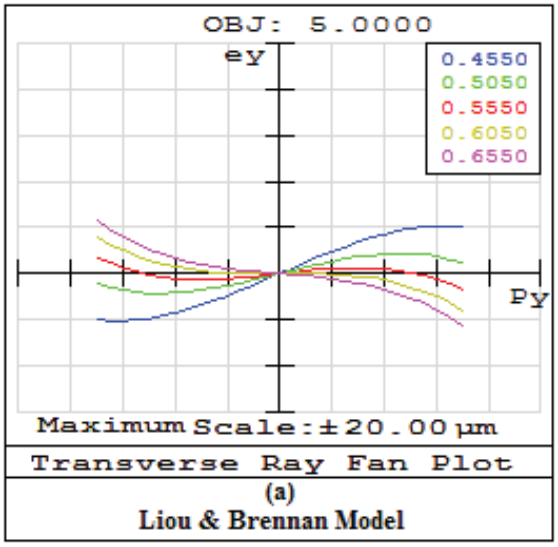

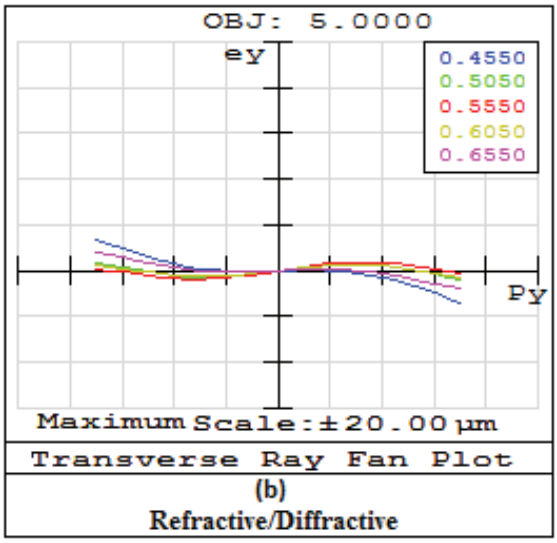

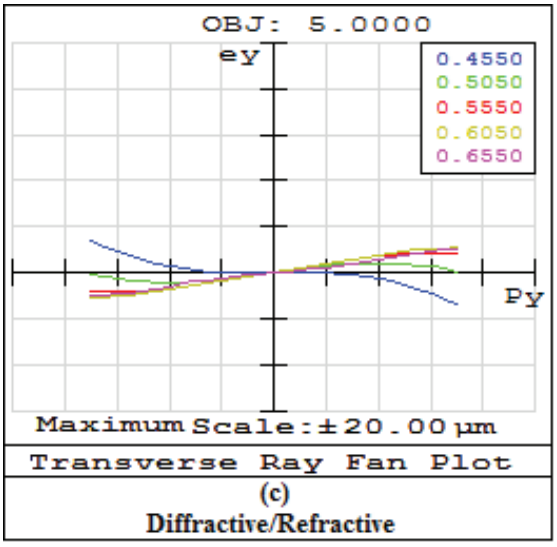

Fig.7. Spherical aberration (color-dependent) of (a) L.&B. model and eye with hybrid MIOLs implanted, (b) R&D model, and (c) D&R model.

4. Conclusion

In this research, the effect of the MOIL surface shape was studied. The MOIL vision efficiency was compared with the healthy eye. The hybrid lens (refraction/diffraction) was implanted instead of the original eye lens (refraction/refraction). The MOIL was examined in two cases; first, the diffraction type surface was positioned as the post surface, and the second surface was the refractive type (D/R), while in the second case, the refractive surface was positioned as a front surface and diffraction as a back surface (R/D).

The MTF, PSF, longitudinal chromatic aberration, and spot diagrams were used as the criteria in this study.

The results show that the MOILs improve the eye

vision since their MTF and PSF are better than those for a healthy eye. Also, for polychromatic light, the longitudinal chromatic aberration (LCA) with hybrid MIOLs is less than that in a healthy eye. It is clear that the use of hybrid MIOLs R/D is more promising case.

ACKNOWLEDGEMENTS

The authors would like to thank Mustansiriyah University (www.uomustansiriyah.edu.iq) and the University of Technology (www.uotechnology.edu.iq) Baghdad, Iraq, for their support in the present work**.**

References

Almeida, M.S.d. & Carvalho, L.A. (2007). Different schematic eyes and their accuracy to the in vivo eye: a quantitative comparison study. Brazilian Journal of Physics, **37**: 378-387.

Alemeddine, O., M. Quinn, A. Qabazard & A. Alhusaini (2002). Trigger synchronization

Barbero, S., Marcos, S., Montejo, J. & Dorronsoro, C. (2011). Design of isoplanatic aspheric monofocal intraocular lenses. Optics express **19**: 6215-6230.

Dandona, L., Dandona, R., Anand, R., Srinivas, M. & Rajashekar, V. (2003). Outcome and number of cataract surgeries in India: policy issues for blindness control. Clinical & experimental ophthalmology **31**: 23-31.

de l'Éclairage, C.I. (1990). CIE 1988 2° spectral luminous efficiency function for photopic vision. Bureau Central de la CIE, Vienna.

Kaiser, P. & Boynton, R. (1996). Human Color Vision. Optical Society of America. Washington, DC.

Kokaj, J., Shuaib, A., Makdisi, Y., Nair, R. & Mathew, J. (2018). Femtosecond laser-based deposition of nanoparticles on a thin film and its characterization. Kuwait Journal of Science 45.

Liou, H.L. & Brennan, N.A. (1997). Anatomically accurate, finite model eye for optical modeling. JOSA A **14**: 1684-1695.

López-Gil, N. & Montés-Micó, R. (2007). New intraocular lens for achromatizing the human eye. Journal of Cataract & Refractive Surgery **33**: 1296-1302.

Olofsson, P., Lundström, M. & Stenevi, U. (2001). Gender and referral to cataract surgery in Sweden. Acta Ophthalmologica Scandinavica **79**: 350-353.

Packer, M., Fine, I.H. & Hoffman, R.S. (2006). Contrast sensitivity and measuring cataract outcomes. Ophthalmol Clin North Am **19**: 521-533.

Pager, C.K., McCluskey, P.J. & Retsas, C. (2004). Cataract surgery in Australia: a profile of patient-centred outcomes. Clinical & experimental ophthalmology, **32**: 388-392.

Siedlecki, D., Zając, M. & Nowak, J. (2007). Characteristics of the retinal images of the eye optical systems with implanted intraocular lenses. Paper presented at: 15th Czech-Polish-Slovak Conference on Wave and Quantum Aspects of Contemporary Optics (International Society for Optics and Photonics).

Siedlecki, D., Zając, M. & Nowak, J. (2008). Retinal images in a model of a pseudophakic eye with classic and hybrid intraocular lenses. Journal of Modern Optics, **55**: 653-669.

Sokolowski, M., Pniewski, J., Brygola, R. & Kowalczyk-Hernandez, M. (2015). Hybrid heptafocal intraocular lenses. Optica Applicata, 45.

Song, H., Yuan, X. & Tang, X. (2016). Effects of intraocular lenses with different diopters on chromatic aberrations in human eye models. BMC ophthalmology, **16**: 9.

Sieburth, R. & Chen, M. (2019). Intraocular lens correction of presbyopia. Taiwan journal of ophthalmology, **9**: 4.

Shaker, M.L., Al-Hamdani H.A. & Al-Amiry A.A. (2020). Nano-particle doped polymers to improve contact lenses optical quality**.** International Journal of Nanoelectronics and Materials, **13**: (1) 19-30.

Wang, J., Candy, T.R., Teel, D.F. & Jacobs, R.J. (2008). Longitudinal chromatic aberration of the human infant eye. JOSA A **25**: 2263-2270.

Weeber, H., Terwee, T., van der Mooren, M. & Piers, P. (2008). Visualization of the retinal image in an eye model with spherical and aspheric, diffractive, and refractive multifocal intraocular lenses. Journal of refractive surgery, **24**: 223-232.

Zając, M. & Nowak, J. (2002). Correction of chromatic aberration in hybrid objectives. Optik, **113**: 299-302.

Zemax, R. (2014). Zemax 13 optical design program user's manual. Zemax LLC. http://www.zemax.com.

Submitted : 29/05/2020
Revised : 13/07/2020
Accepted : 14/072020
DOI : 10.48129/kjs.v48i1.9841